OPEN

Interhemispheric Auditory Cortical Synchronization in Asymmetric Hearing Loss

Jolie L. Chang,[1] Ethan D. Crawford,[1] Abhishek S. Bhutada,[2] Jennifer Henderson Sabes,[1] Jessie Chen,[2] Chang Cai,[2] Corby L. Dale,[2] Anne M. Findlay,[2] Danielle Mizuiri,[2] Srikantan S. Nagarajan,[1,2] and Steven W. Cheung[1]

Objectives: Auditory cortical activation of the two hemispheres to monaurally presented tonal stimuli has been shown to be asynchronous in normal hearing (NH) but synchronous in the extreme case of adult-onset asymmetric hearing loss (AHL) with single-sided deafness. We addressed the wide knowledge gap between these two anchoring states of interhemispheric temporal organization. The objectives of this study were as follows: (1) to map the trajectory of interhemispheric temporal reorganization from asynchrony to synchrony using magnitude of interaural threshold difference as the independent variable in a cross-sectional study and (2) to evaluate reversibility of interhemispheric synchrony in association with hearing in noise performance by amplifying the aidable poorer ear in a repeated measures, longitudinal study.

Design: The cross-sectional and longitudinal cohorts were comprised of 49 subjects (AHL; N = 21; 11 male, 10 female; mean age = 48 years) and NH (N = 28; 16 male, 12 female; mean age = 45 years). The maximum interaural threshold difference of the two cohorts spanned from 0 to 65 dB. Magnetoencephalography analyses focused on latency of the M100 peak response from auditory cortex in both hemispheres between 50 msec and 150 msec following monaural tonal stimulation at the frequency (0.5, 1, 2, 3, or 4 kHz) corresponding to the maximum and minimum interaural threshold difference for better and poorer ears separately. The longitudinal AHL cohort was drawn from three subjects in the cross-sectional AHL cohort (all male; ages 49 to 60 years; varied AHL etiologies; no amplification for at least 2 years). All longitudinal study subjects were treated by monaural amplification of the poorer ear and underwent repeated measures examination of the M100 response latency and quick speech in noise hearing in noise performance at baseline, and postamplification months 3, 6, and 12.

Results: The M100 response peak latency values in the ipsilateral hemisphere lagged those in the contralateral hemisphere for all stimulation conditions. The mean (SD) interhemispheric latency difference values (ipsilateral less contralateral) to better ear stimulation for three categories of maximum interaural threshold difference were as follows: NH (≤ 10 dB)—8.6 (3.0) msec; AHL (15 to 40 dB)—3.0 (1.2) msec; AHL (≥ 45 dB)—1.4 (1.3) msec. In turn, the magnitude of difference values were used to define interhemispheric temporal organization states of asynchrony, mixed asynchrony and synchrony, and synchrony, respectively. Amplification of the poorer ear in longitudinal subjects drove interhemispheric organization change from baseline synchrony to postamplification asynchrony and hearing in noise performance improvement in those with baseline impairment over a 12-month period.

Conclusions: Interhemispheric temporal organization in AHL was anchored between states of asynchrony in NH and synchrony in single-sided deafness. For asymmetry magnitudes between 15 and 40 dB, the intermediate mixed state of asynchrony and synchrony was continuous and reversible. Amplification of the poorer ear in AHL improved hearing in noise performance and restored normal temporal organization of auditory cortices in the two hemispheres. The return to normal interhemispheric asynchrony from baseline synchrony and improvement in hearing following monoaural amplification of the poorer ear evolved progressively over a 12-month period.

Key words: Asymmetric hearing loss, Asynchrony, Hearing aid, Interaural, Interhemispheric, Magnetoencephalography, Threshold.

Abbreviations: AHL = asymmetric hearing loss; dB = decibel; IRB = Institutional Review Board; kHz = kiloHertz; MEGI = magnetoencephalographic imaging; mm = millimeter; MNI = Montreal Neurological Institute; MRI = magnetic resonance imaging; msec = millisecond; N = number of samples; NH = normal hearing; pT = picoTesla; SD = standard deviation; SSD = single-sided deafness.

(Ear & Hearing 2021;42;1253–1262)

INTRODUCTION

Adult-onset asymmetric hearing loss (AHL) most commonly arises from directional acoustic trauma, sudden hearing loss, endolymphatic hydrops, and retrocochlear lesions. AHL clinical consequences are evident on tasks that require localizing sound sources in space (Noble & Gatehouse 2004; Douglas et al. 2007), where the degradation to spatial hearing is related to the magnitude of sensitivity difference between the two ears (Chang et al. 2020) and hearing speech in noise, where the monaural listener will bear a 9 dB disadvantage for the dichotic condition of signal to the poorer ear and noise to the better ear (Vannson et al. 2015). Beyond those clinical impairments, the poorer ear in AHL is at risk for accelerated decline from auditory deprivation (Silman et al. 1984; Silverman & Emmer 1993; Silverman et al. 2006). In audiometrically well-matched cohorts with moderate AHL and maximum interaural threshold difference of ~40 dB between 2 and 4 kHz, the speech recognition scores of the poorer ear in the cohort without amplification showed significant decline over a 2-year period (Silverman et al. 2006). Remarkably, the deleterious effects of auditory deprivation can be reversed by amplification of the poorer ear (Silverman & Emmer 1993). While cross-sectional and longitudinal audiological AHL studies have yielded clinical insights, the central neurophysiological bases of untreated and treated AHL hearing performance outcomes remain largely unknown.

Human neuroimaging studies on adult-onset AHL in the extreme case of single-sided deafness (SSD) have nonetheless provided specific information on change in the relative timing of

[1]Department of Otolaryngology-Head and Neck Surgery, University of California, San Francisco, California, USA; and [2]Department of Radiology and Biomedical Imaging, University of California, San Francisco, California, USA.

auditory cortical activation across the two hemispheres to advance research in this area. In normal hearing (NH), monaural sound presentation using functional magnetic resonance imaging (MRI) (Scheffler et al. 1998) and evoked potential imaging (Fujiki et al. 1998) techniques showed stronger activation strength in the contralateral hemisphere relative to the stimulated ear and asynchronous activation timing across the two hemispheres. In contrast, monaural sound presentation to the only hearing ear in adult-onset SSD demonstrated comparable activation strengths and nearly synchronous activation timing across the two hemispheres (Bilecen et al. 2000; Ponton et al. 2001). Interhemispheric auditory cortical asynchrony in NH and synchrony in SSD are supported by parallel findings in animal studies (Kitzes & Semple 1985; Reale & Kettner 1986; Popelar et al. 1994; Lee et al. 2017).

Interhemispheric auditory cortical synchrony in adult-onset SSD has been quantified using magnetoencephalography (MEG) imaging. The latency of the M100 peak in the ipsilateral hemisphere relative to the stimulated ear lags behind its counterpart in the contralateral hemisphere. The interhemispheric peak latency difference (ipsilateral minus contralateral) declines from predominant asynchrony at 6.6 milliseconds (msec) in NH to relative synchrony at 1.7 msec in SSD (Pross et al. 2015). Interhemispheric temporal organization in AHL appears to be bracketed by two brain states: asynchrony in normal binaural hearing and synchrony in SSD with obligatory monaural hearing. The neuroimaging and clinical knowledge gap of intermediate AHL audiometric profiles with a poorer ear responsive to sound stimulation is considerable and understudied.

Informed by anchoring data from NH and SSD, we probed auditory cortical interhemispheric synchronization by measuring the M100 interhemispheric peak latency difference along a continuum of AHL interaural threshold difference magnitudes in subjects with acoustically responsive poorer ears. The objectives of this article were twofold: (1) to map the trajectory of interhemispheric temporal reorganization from asynchrony to synchrony using magnitude of interaural threshold difference as the independent variable in a cross-sectional study and (2) to evaluate reversibility of interhemispheric synchrony in association with hearing in noise performance by amplifying the aidable poorer ear in a repeated measures, longitudinal study.

MATERIALS AND METHODS

Subjects

The AHL cohort was comprised of 21 subjects (11 males, 10 females), with mean age at 48 years (range: 29 to 74 years). The better ear was the right in nine subjects and left in 12 subjects. The NH cohort was comprised of 28 subjects (16 males, 12 females), with mean age at 45 years (range: 23 to 64 years). There were no differences in age or sex in pairwise comparisons of the two cohorts. Better ear and poorer ear distinction in the NH cohort was not applicable. The AHL cohort mean hearing loss duration was 3.2 years and audiometric thresholds from 0.5 to 8 kHz showed the better ear had mild loss and the poorer had moderate loss for frequencies ≥ 4 kHz (Table 1). The maximum interaural threshold difference of the two cohorts spanned from 0 to 65 dB. This study was conducted in accordance with the Declaration of Helsinki. The University of California San Francisco Institutional Review Board approved all study procedures (IRB No. 13-10671). All participants provided verbal and written informed consent before enrollment.

TABLE 1. Asymmetric hearing loss and normal-hearing cohorts

Cohort	Asymmetric hearing loss	Normal hearing
No. subjects	21	28
Sex, male:female	11:10	16:12
Age, mean (range), yr	48 (29–74)	45 (23–64)
BE, right:left	9:12	N/A
Duration of hearing loss, mean (range), yr	3.2 (0.2–10)	N/A
Audiometric threshold mean (95% CI)		
0.5 kHz	15 (10–19) BE	9 (7–11) RE
	40 (31–48) PE	8 (6–10) LE
1.0 kHz	14 (10–17) BE	8 (5–10) RE
	44 (35–53) PE	8 (5–10) LE
2.0 kHz	14 (8–19) BE	8 (5–11) RE
	47 (41–54) PE	9 (5–12) LE
3.0 kHz	19 (12–26) BE	9 (6–12) RE
	50 (42–58) PE	7 (4–10) LE
4.0 kHz	20 (13–28) BE*	6 (4–9) RE
	48 (40–56) PE	6 (3–9) LE
6.0 kHz	25 (15–35) BE*	9 (7–12) RE
	54 (44–63) PE	9 (7–12) LE
8.0 kHz	26 (15–38) BE*	11 (8–14) RE
	51 (40–61) PE	13 (10–17) LE

Normal hearing cohort RE and LE 95% audiometric threshold CIs overlap at all frequencies; no BE and PE distinction.

**Asymmetric hearing loss cohort BE has mild hearing loss compared with the normal hearing cohort, where CIs do not overlap at 4 kHz, 6 kHz, and 8 kHz.*

BE, better ear; CI, confidence interval; kHz, kiloHertz; LE, left ear; PE, poorer ear; RE, right ear.

Experimental Designs and Cohorts

This study on adult subjects was conducted using two experimental designs. The first design was cross-sectional contrast of AHL and NH cohorts to examine the relationship between M100 interhemispheric latency difference and interaural threshold difference at three categorical levels of audiometric asymmetry. The second design was longitudinal tracking of changes to M100 interhemispheric latency difference and hearing in noise performance in three AHL subjects who were monaurally amplified with an extended wear hearing aid (Lyric) to the poorer ear. Inclusion criteria included the following audiometric definitions (Margolis & Saly 2008): (1) AHL: ≥ 15 dB interaural threshold difference across two or more adjacent frequencies for 0.5, 1, 2, 3, and 4 kHz and (2) NH: ≤ 10 dB interaural threshold difference across two or more adjacent frequencies for 0.5, 1, 2, 3, and 4 kHz and ≤ 20 dB threshold at 0.5, 1, 2, 3, 4, 6, and 8 kHz in both ears. The AHL cutoff at 4 kHz was designed to capture the most robust and reliable auditory evoked response signals using MEG.

MRI Anatomical and MEG Data Acquisition

Structural MRI data were acquired from each subject on a 3T MRI scanner (Discovery MR750; GE Medical system, Waukesha, WI). T1-weighted fast spoiled gradient-echo recalled brain volume scans were obtained (120 axial slices, field of view = 512 mm × 512 mm, repetition time = 7232 msec, echo time = 2.78 msec, in-plane voxel dimensions 0.5 × 0.5 mm^2, slice thickness = 1.5 mm). MEG recordings were performed in a magnetically shielded room housing a 275-channel whole-head axial neuromagnetometer (CTF Omega 2000; VSM MedTech). Pure-tone sound stimuli at 0.5, 1, 2, 3, and 4 kHz (stimuli: 400 msec duration with 25 msec ramp up and down, 120 trials) were presented monaurally, without amplification in

all subjects. MEG stimulus intensity levels to both ears ranged typically between 15 and 40 dB sensation level at 1 kHz of the better ear, based on hearing comfort.

MEG Data Preprocessing

MEG data were 3rd order gradient denoised, detrended, and filtered from 4 to 40 Hz. MEG sensor data for 120 trials of each condition were averaged after rejection of trials with artifacts due to respiratory, eye or jaw movement that exceed 1 pT in any sensor. Each structural MRI scan was coregistered to MEG data using anatomical points matched to fiducial markers on the tragus and the nasion. This was performed by applying averaged MEG sensor data to spatially normalized (Montreal Neurological Institute [MNI] atlas template) MRI scans. We used the Neurodynamic Utility Toolbox for Magnetoencephalography open-source analysis toolbox in MATLAB to calculate a three-component lead-field for each voxel by applying a forward model of sensor activity at a spatial resolution of 5 mm, spanning the entire brain (Dalal et al. 2008; Dalal et al. 2011; Owen et al. 2012). Since MEG sensors located outside the scalp measured distant neural signals, estimation of spatiotemporal activity in the brain required use of a robust signal source localization algorithm. We deployed Champagne for spatial localization and time course estimation of neuroimaging data derived from complex brain source configurations (Wipf et al. 2010; Owen et al. 2012). In contrast to parametric dipole fitting procedures that required expert manual selection of a single time-point for operator-dependent localization of signal source within each hemisphere separately, Champagne performed automated localization of spatiotemporal cortical activity for the entire auditory evoked field data time-series in both hemispheres consistently (Niziolek et al. 2013; Cai et al. 2019).

MEG Data Analysis

We localized and reconstructed spatiotemporal neural activity in the auditory cortices of both hemispheres using MEG data captured between 25 and 250 msec following stimulus presentation. Activation patterns were displayed on the MNI brain template for visual confirmation of auditory cortical origin. Tri-planar MNI coordinates of the voxel corresponding to M100 response peaks were identified for ipsilateral and contralateral auditory cortical hemispheres relative to the stimulated ear (randomly chosen ear in NH, better or poorer ear in AHL). The root mean square time course of source activity from those voxel coordinates were estimated in the two auditory cortices. The primary MEG metric, latency of the M100 peak response between 50 and 150 msec following stimulus onset (Pross et al. 2015; Chang et al. 2016), was extracted at the frequency corresponding to the maximum and minimum interaural threshold difference for better and poorer ears separately.

Hearing in Noise Performance

Three subjects in the AHL cohort underwent monaural amplification of the poorer ear, which was fitted with an in-the-ear (Lyric) extended wear (2 to 3 months) hearing aid to promote around-the-clock use. Hearing in noise performance using the quick speech in noise (QuickSIN) test (normal < 3, higher score denotes poorer function) (Killion et al. 2004) and MEG assessments were documented at baseline, and post-treatment months 3, 6, and 12. Other audiological assessments included pure-tone audiometry and Northwestern University Auditory Test No. 6 word recognition score at baseline and post-treatment month 12.

Statistical Analyses

Analyses included descriptive statistics of demographic and audiometric data, statistical inference tests, and correlation examinations of MEG data. Interhemispheric latency difference was calculated by subtracting the M100 latency in the contralateral auditory cortex relative to ear stimulation from the M100 latency in the ipsilateral auditory cortex for monaurally presented tonal stimuli at 0.5, 1, 2, 3, and 4 kHz. The interaural threshold difference was computed at 0.5, 1, 2, 3, and 4 kHz to determine the frequencies of maximum and minimum difference.

RESULTS

M100 Response Activation Peak

Interhemispheric response asynchrony showed relatively longer ipsilateral cortical response latency times to tonal stimuli. MEG sensor data time-series waveforms of the dominant M100 response occurred in the 50 msec to 150 msec window following stimulus onset, which was preceded or succeeded by a weaker response (Fig. 1, left column). Brain source localization of spatiotemporal MEG data using the Champagne algorithm identified peaks from auditory cortex in the two hemispheres (Fig. 1, colored dots within coronal plane MRI insets, right column) and captured the auditory cortical signal time-series waveform (Fig. 1, right column). The root mean square peak M100 latency value for each hemisphere was extracted from this time-series waveform to record absolute and to calculate difference (ipsilateral less contralateral) values. The M100 latency was longer in the ipsilateral hemisphere compared with the contralateral hemisphere in both subjects, NH (Fig. 1B, D) and AHL (Fig. 1F, H), but the interhemispheric latency difference was more pronounced in NH (Fig. 1, dashed lines, right column).

Interhemispheric Latency and Interaural Threshold Differences

Cohort Comparisons • The M100 response peak latency values in the ipsilateral hemisphere lagged those in the contralateral hemisphere for all stimulation conditions (Fig. 2). Contralateral and ipsilateral hemisphere was defined relative to the stimulated ear. For the NH cohort, better and poorer ear distinction was not applicable, so one ear was randomly chosen was report M100 latency. The NH cohort mean (SD) ipsilateral latency was 108.0 (8.6) msec and contralateral latency was 99.4 (7.2) msec. For better ear stimulation in the AHL cohort, the mean ipsilateral latency was 102.3 (15.6) msec and contralateral latency was 100.1 (15.3) msec. For poorer ear stimulation in the AHL cohort, the mean ipsilateral latency was 104.3 (9.7) msec and contralateral latency was 99.9 (10.1) msec. The AHL cohort exhibited decreased ipsilateral latency to both better and poorer ear stimulation compared with the NH cohort, but the magnitude was more pronounced for better ear stimulation.

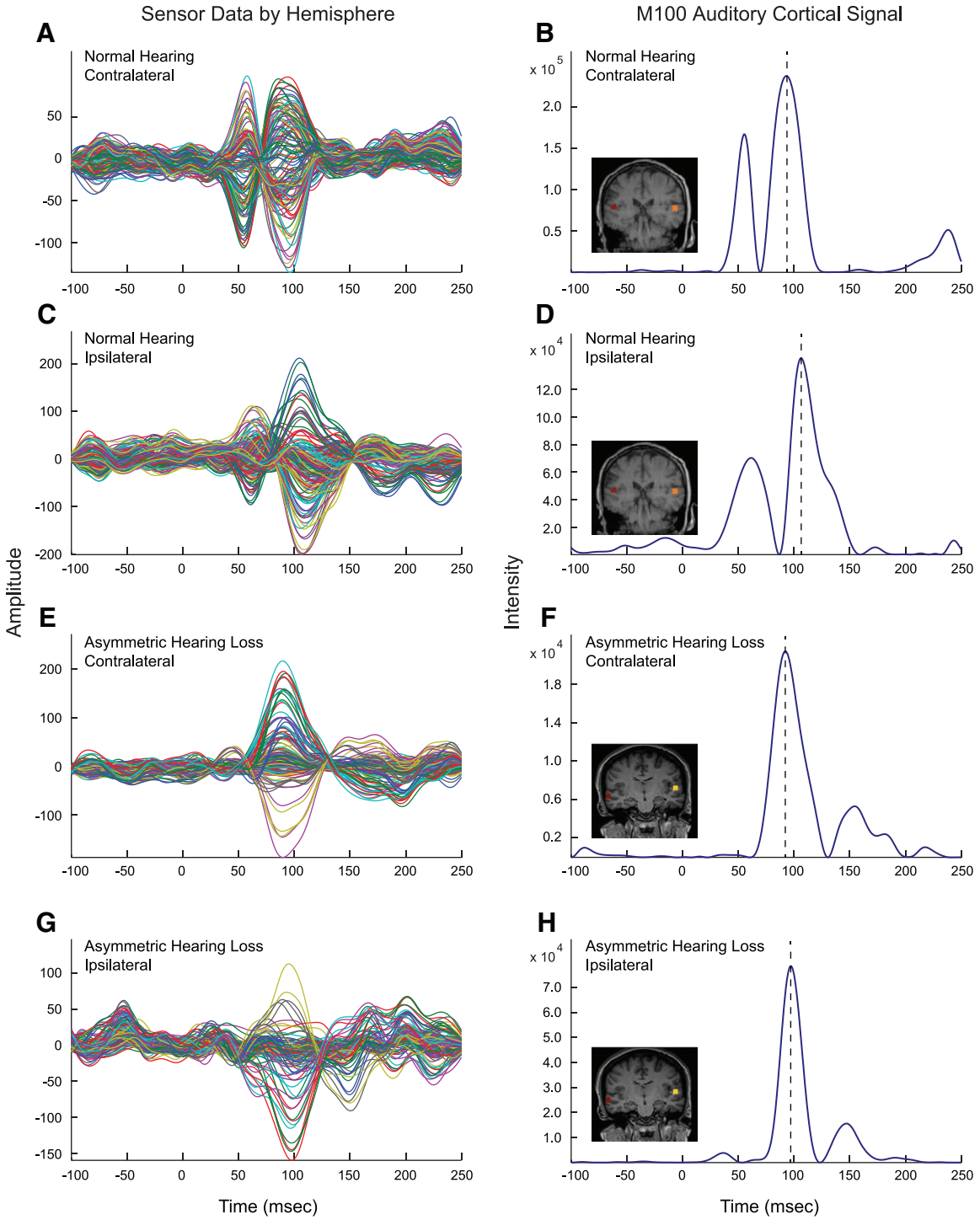

Fig. 1. Raw MEG sensor data and M100 peak source localization from normal hearing and asymmetric hearing loss subjects. Left column, MEG data traces by hemisphere relative to the stimulated ear. Right column, M100 response peak localization to auditory cortex (MRI insets) and latency determination (dashed lines). Interhemispheric latency difference is greater for the normal hearing subject. MEG indicates magnetoencephalography; MRI, magnetic resonance imaging.

The interhemispheric M100 response peak latency difference values (ipsilateral less contralateral) were lower in the AHL cohort (Fig. 3). For the NH cohort, the mean latency difference was 8.6 (3.0) msec. For the AHL cohort, better ear and poorer ear latency difference values were calculated at stimulation frequencies corresponding to the minimum and maximum interaural threshold difference. The mean (SD) AHL interhemispheric latency difference values were as follows: (A) better ear stimulation: 5.3 (2.1) msec at minimum and 2.2 (1.4) msec at maximum and (B) poorer ear stimulation: 5.8 (2.2) msec at minimum and 4.9 (3.3) msec at maximum. It is interesting that range of latency differences (Tukey boxplots show 10th and 90th percentile, Fig. 3) was lowest for AHL better ear stimulation at maximum interaural threshold difference. Interhemispheric latency

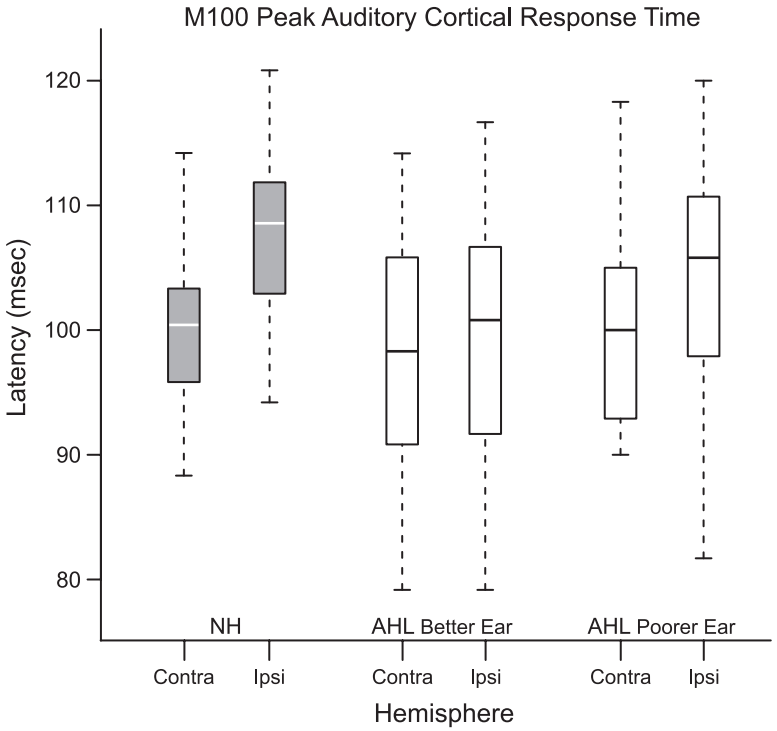

Fig. 2. M100 auditory cortical response latency in the hemisphere referenced to the stimulated ear. M100 median latencies in the NH cohort are 100.4 msec (contralateral) and 108.6 msec (ipsilateral) and AHL cohort are 98.3 msec (contralateral, better ear), 100.8 msec (ipsilateral, better), 100.0 msec (contralateral, poorer ear), and 105.8 msec (ipsilateral, poorer ear). Ipsilateral cortical response latency to both better and poorer ear stimulation in the AHL cohort is shorter compared with the NH cohort. Tukey boxplots truncated at the 10th and 90th percentiles. AHL indicates asymmetric hearing loss; Contra, contralateral; Ipsi, ipsilateral; NH, normal hearing.

differences were significant ($p < 0.001$, t test with Bonferroni correction) in pairwise comparisons with the NH cohort for all four AHL cohort stimulation conditions.

Interhemispheric cortical response asynchrony was disrupted monotonically in AHL. Within the AHL cohort, interhemispheric latency difference was examined for two maximum interaural threshold difference categories, 15 to 40 dB and ≥ 45 dB. The mean (SD) difference values were 3.0 (1.2) msec in the 15 to 40 dB and 1.4 (1.3) msec in the ≥ 45 dB categories, respectively. Interhemispheric latency difference and AHL duration correlation was not significant on linear regression analysis ($p = 0.23$). Interhemispheric latency difference in pairwise comparisons of all three categories of maximum interaural threshold asymmetry were significant ($p = 0.05$, t test with Bonferroni correction), where the difference value was largest for NH (≤ 10 dB), intermediate for AHL (15 to 40 dB), and smallest for AHL (≥ 45 dB).

Frequency Specificity of Interhemispheric Synchrony • Interhemispheric synchronization in AHL hearing loss was focally specific to the frequency at maximum interaural threshold difference. To examine focality of interhemispheric synchrony or the minimum interhemispheric latency difference within single subjects, we analyzed nine subjects in the AHL cohort where maximum and minimum interaural threshold differences were separated by at least 15 dB. Interhemispheric latency difference data for this AHL subgroup were plotted against neighboring frequencies surrounding the reference frequency at maximum interaural threshold difference (Fig. 4). There was increasing asynchrony or growing interhemispheric latency difference for lower and higher neighborhood frequencies that were farther away from the frequency at maximum. Using the criterion of two neighborhood frequencies away from the frequency at maximum as endpoint measurements, both lower (N = 6) and higher (N = 7) endpoint frequencies showed increased asynchrony with higher difference values ($p = 0.05$, Wilcoxon signed-rank test). Four of nine subjects reached ~8 msec, approaching the mean value of interhemispheric latency difference in the NH cohort (8.6 msec). In notch shaped AHL pattern, interhemispheric synchrony was focal to the frequency at maximum interaural threshold difference. As the interaural threshold difference narrowed at successive frequencies farther away from the frequency at maximum, there was return to more normal interhemispheric latency difference values and reestablishment of interhemispheric asynchrony.

Reversal of Interhemispheric Synchrony and Hearing in Noise Improvement

Monaural amplification of the poorer ear in AHL restored interhemispheric asynchrony and improved hearing in noise performance. Three subjects in the AHL cohort were treated by monaural amplification of the poorer ear. The age, sex, chronicity, and etiology of AHL in the longitudinal study cohort were as follows: (A) R1940—58-year-old man with a 1.3-year history of right ear sudden hearing loss that was unresponsive to medical therapy, (B) R1961—49-year-old man with a 2-year history of poorer hearing in the left ear of uncertain etiology, and (C) R2006—60-year-old man with a 10-year

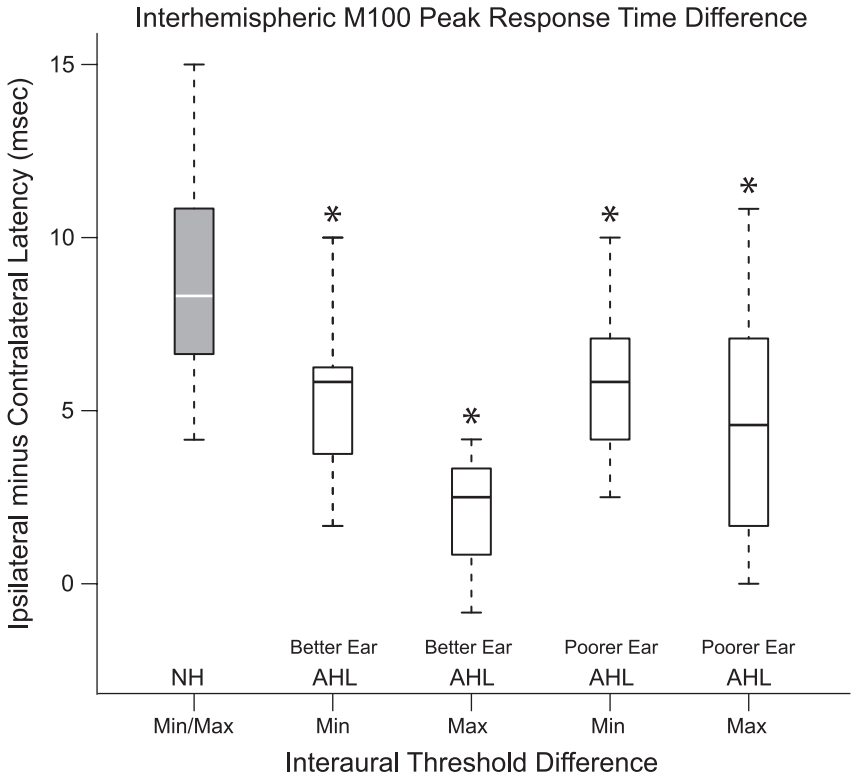

Fig. 3. M100 interhemispheric latency difference referenced to stimulation at the frequency corresponding to minimum (min) and maximum (max) interaural threshold difference. The min and max interaural threshold difference in the NH cohort is essentially identical, denoted by min/max. M100 median interhemispheric difference latencies in the NH cohort are 8.3 msec and AHL cohort are 5.8 msec (min, better ear), 2.5 msec (max, better), 5.8 msec (min, poorer ear), and 4.6 msec (max, poorer ear). Using NH cohort as the comparator, pairwise comparisons show all four AHL interhemispheric latency differences are smaller ($p < 0.001$, t test with Bonferroni correction, denoted by *). Tukey boxplots truncated at the 10th and 90th percentiles. AHL indicates asymmetric hearing loss; max, maximum interaural threshold difference; min, minimum interaural threshold difference; NH, normal hearing.

history of endolymphatic hydrops limited to the right ear that stabilized to a higher audiometric thresholds without fluctuation 3 years ago. Amplification had not been considered by R1940 and R2006, and abandoned by R1961 after a brief trial 2 years prior. The maximum interaural threshold asymmetry (Fig. 5A–C) was wide (> 40 dB) in R1940 and R2006, and narrow (15 to 20 dB) in R1961. Interhemispheric latency differences determined by better and poorer ear stimulation at maximum showed steady progression toward values expected of normal-hearing subjects over a 12-month period of monaural amplification. The interval latency difference change from baseline to month 12 by stimulation ear were as follows: R1940 (9.2 msec, better ear; 10.0 poorer ear), R1961 (5.9 msec, better ear; 5.8 msec poorer ear), and R2006 (5.8 msec, better ear; 8.3 msec poorer ear). Interhemispheric temporal organization reversed from baseline synchrony to asynchrony in all subjects following increased activity of the poorer ear in AHL (Fig. 5D, E). Hearing in noise performance of the poorer ear in the two subjects (R1940, R2006) with reduced baseline performance and concurrent wide maximum interaural threshold asymmetry showed improvement by post-treatment month 6 (Fig. 5F). Demonstration of hearing in noise improvement in the poorer ear of R1961 and all better ears was not possible due to normal performance at baseline (< 3 score on QuickSIN). Pure-tone thresholds and recognition scores of all better and poorer ears at post-treatment month 12 were not significantly different from baseline (Carney & Schlauch 2007). This repeated measures, longitudinal experiment showed increased activity of the poorer ear was accompanied by neurophysiological and clinical changes. Interhemispheric temporal organization reversed from synchrony to asynchrony and hearing in noise performance improved in the two ears without measurement floor effect.

DISCUSSION

We demonstrate the M100 interhemispheric latency difference is monotonically dependent on the magnitude of maximum interaural threshold difference across three categories of asymmetry: NH (≤ 10 dB), AHL (15 to 40 dB), and AHL (≥ 45 dB). While the change from asynchrony to synchrony in interhemispheric temporal organization has previously been demonstrated for the AHL extreme case of SSD with an unresponsive poorer ear (Fujiki et al. 1998; Ponton et al. 2001; Pross et al. 2015; Lee et al. 2017), there is a paucity of information on AHL with an acoustically responsive poorer ear. We begin to address this knowledge gap by probing the continuum of interhemispheric temporal organization in subjects with audiometric asymmetry that span from 0 to 65 dB. Interhemispheric auditory cortical synchronization in AHL is dependent on magnitude of interaural threshold asymmetry, and may be focal and frequency specific. Interhemispheric temporal states may be classified in the following manner: asynchrony in NH, synchrony in AHL ≥ 45 dB, and intermediate mixed asynchrony and synchrony in AHL 15 to 40 dB.

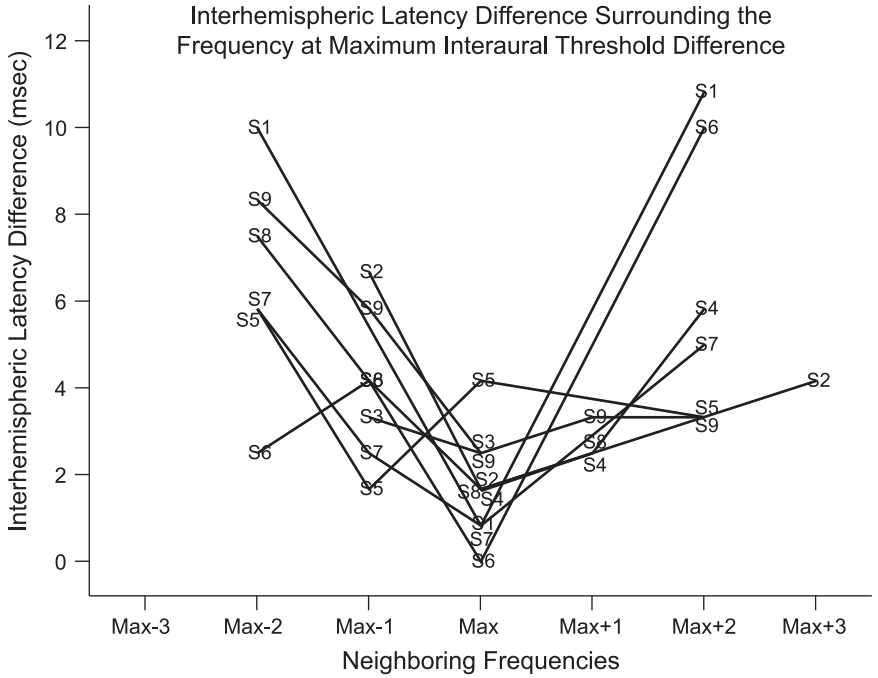

Fig. 4. M100 interhemispheric latency difference surrounding the frequency at maximum interaural threshold difference in notched AHL audiometric profile. *X* axis indicates the number of frequency steps away from the frequency at maximum interaural threshold difference. Interhemispheric latency difference values increase at lower and higher frequencies away from the minimum interhemispheric latency value at maximum interaural threshold difference ($p = 0.05$, Wilcoxon signed-rank test). Interhemispheric synchrony is focal to the frequency at maximum interaural threshold difference in notch shaped AHL pattern. Letter symbols are used to denote individual subjects. AHL indicates asymmetric hearing loss.

The M100 latency difference value of 1.4 msec for the AHL ≥ 45 dB category is comparable to 1.7 msec reported for the AHL extreme case of SSD (Pross et al. 2015) and suggests ≥ 45 dB sensitivity difference between the two ears may demarcate the cutoff for functional SSD despite an acoustically responsive poorer ear. In this regard, a recent study on ear preference and interaural threshold asymmetry shows preference strength for the better ear is monotonically dependent on magnitude of asymmetry and the AHL ≥ 45 dB category is associated with the most severe impairment in spatial hearing (Chang et al. 2020), similar to SSD following acoustic neuroma surgery (Douglas et al. 2007). Taken together, interhemispheric temporal states of asynchrony and synchrony are bracketed by NH and AHL with anatomical or functional SSD.

Interhemispheric temporal states are dynamic and activity-based plasticity mechanisms may be important in shaping cortical plasticity. Increasing auditory activity to an aidable poorer ear by fitting a hearing device drives interhemispheric temporal reorganization toward normal asynchrony and improves hearing in noise performance. By post-treatment month 12, all three subjects exhibit complete or nearly complete return to normal interhemispheric asynchrony from baseline synchrony for better ear and poorer ear stimulation at the maximum interaural threshold difference. At post-treatment month 6, the two subjects with demonstrable hearing in noise impairment at baseline improved performance. It should be noted that R1961, the subject without baseline hearing in noise impairment on QuickSIN and with the narrowest maximum interaural threshold asymmetry (15 to 20 dB), shows the fastest improvement toward interhemispheric asynchrony upon monaural amplification. Findings from the repeated measures, longitudinal study are internally consistent with the cross-sectional cohort contrast study of this project. Greater interhemispheric asynchrony is observed with narrower functional interaural threshold asymmetry magnitude conferred by monaural amplification of the poorer ear. The M100 interhemispheric latency difference measure may be interrogated in future studies to evaluate its suitability to serve as a treatment responsive biomarker in AHL patients with baseline impairments in hearing in noise and other evaluable clinical domains.

The neurophysiological bases of interhemispheric temporal plasticity and activity-based hearing performance improvement of the amplified poorer ear are unknown. There are rich sets of possible interactions among central and peripheral auditory stations that subserve binaural hearing, posing a considerable challenge to specify the key ones that could account for dependencies on interaural threshold difference and poorer ear stimulation. Given the very limited information on this topic, we can offer a conceptual framework to test plausible hypotheses in future investigations.

Normal mirror-image functional organization to tonal stimuli across the two hemispheres is disrupted in AHL. The contralateral hemisphere realigns the interaural frequency map by elevating cortical thresholds and the ipsilateral hemisphere retains cortical sensitivity without realigning the frequency map (Cheung et al. 2009; Cheung et al. 2017). This release from corticocortical alignment of representation maps is referred to as anisomorphic cortical reorganization, which may alter interhemispheric temporal synchrony through modulation of callosal functional connectivity. Interhemispheric asynchrony in NH reflects transfer time (Henshall et al. 2012; Scally et al. 2018) for a signal to cross from contralateral to ipsilateral auditory cortex via modular callosal connections (Code & Winer 1986; Rouiller

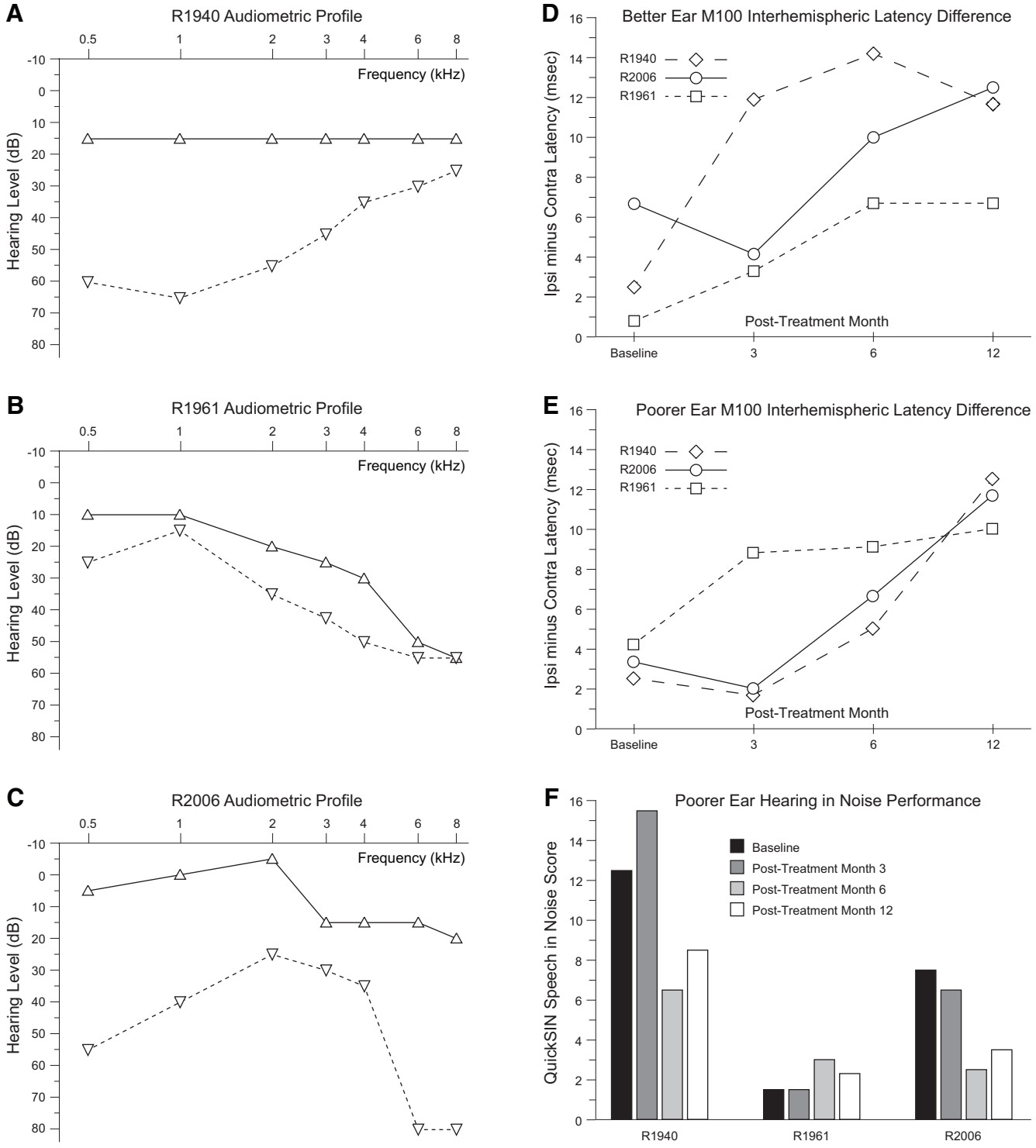

Fig. 5. Reversal of the M100 interhemispheric latency difference from synchrony to asynchrony and hearing in noise improvement in three AHL subjects treated by monaural amplification of the poorer ear. Assessments at baseline, and months 3, 6, and 12 following poorer ear amplification are exhibited. A–C, Audiometric profiles of the three subjects. D and E, M100 interhemispheric latency difference values show steady progression toward values expected of normal-hearing subjects over a 12 mo period of monaural amplification. Interhemispheric temporal organization reverses from synchrony to asynchrony by increasing activity of the poorer ear in AHL. F, Poorer ear hearing in noise performance improvement is evident at month 6 and plateaus thereafter in the two subjects (R1940 and R2006) with abnormal baseline performance. AHL indicates asymmetric hearing loss; QuickSIN, quick speech in noise.

et al. 1991). In an excitatory model of corpus callosum function, where information reinforcement and hemispheric integration are critical features (Kinsbourne 1970; Guiard 1980; Yazgan et al. 1995; Bloom & Hynd 2005; van der Knaap & van der Ham 2011), these transcallosal signals may assist with decision-making on uncertain sound objects, such as those embedded in noise.

Consistent with this notion, there is reduction of corpus callosum white matter integrity in SSD (Shang et al. 2018), the extreme case of AHL with irreversible interhemispheric synchrony.

Anisomorphic cortical reorganization (Cheung et al. 2017) may also change interhemispheric synchrony through alteration of corticofugal outflow to the inferior colliculi, a station with extensive commissural connections that can influence the hemispheric distribution of auditory information (Saldaña & Merchán 2005). This may reduce activation of intrinsically inhibitory GABAergic inferior colliculus networks (Popelář et al. 2016) and enable earlier delivery of ascending auditory pathway signals (Kitzes & Semple 1985) to ipsilateral auditory cortex, thereby reducing interhemispheric latency difference values and disrupting the corticocortical signal query system. This alteration to corticofugal modulation of ascending auditory inputs could be a neurophysiological basis of ear preference in AHL (Chang et al. 2020). As interhemispheric signal transfer decreases due to alterations in either transcallosal or corticofugal pathways, the range of interhemispheric latency difference also decreases and preference strength for the better ear increases. This may account for the observed lowest range of interhemispheric latency difference under the condition of better ear stimulation at maximum interaural threshold difference (Fig. 3).

A limitation of this study is focus on the better ear for determining interhemispheric latency difference, where stimulation intensity levels for both ears are determined solely by the loudest comfortable hearing level of the better ear at 1 kHz. A responsive poorer ear in this AHL cohort allows for comparison of results for better and poorer ear stimulation. While qualitatively similar, results appear to differ quantitatively in effect size. As relatively lower stimulation intensity levels may impact poorer ear MEG data, a study with stimulation intensity adjusted for each ear separately will be necessary to address interhemispheric organization to poorer ear stimulation more rigorously.

CONCLUSIONS

Interhemispheric temporal organization is anchored by states of asynchrony in NH and synchrony in SSD. For asymmetry magnitudes between 15 and 40 dB, the intermediate mixed state of asynchrony and synchrony is continuous and reversible. Amplification of the poorer ear in AHL improves hearing in noise performance and restores normal temporal organization of auditory cortices in the two hemispheres. The return to normal interhemispheric asynchrony from baseline synchrony and improvement in hearing following monoaural amplification of the poorer ear evolves progressively over a 12-month period.

ACKNOWLEDGMENTS

The authors thank the Phonak Corporation for donating the Lyric hearing aids used in this study free of charge. Phonak did not participate in study design, data analyses, or writing of the article.

This work was supported by Department of Defense grants W81XWH1310494 and W81XWH1810741, National Institutes of Health National Institutes of Health (NIH)/National Institute on Deafness and Other Communication Disorders 1R01DC017396, NIH/National Center for Advancing Translational Sciences University of California, San Francisco-Clinical and Translational Science Institute UL1 TR000004, The Triological Society, Hearing Research, Inc, and the Coleman Memorial Fund.

The authors have no conflicts of interest to disclose.

J.L.C. designed experiments, acquired and analyzed data, and drafted the article. E.D.C, A.S.B., J.H.-S., J.C., C.C., C.L.D., and A.M.F. analyzed and interpreted data. D.M. acquired data. S.S.N. designed experiments and interpreted data. S.W.C. designed experiments, interpreted data, and revised article critically for content. All authors discussed the results and implications, commented on the article at all stages, and approved the final version for publication.

Address for correspondence: Steven W. Cheung, UCSF Otolaryngology, Division of Otology, Neurotology, and Skull Base Surgery, 2233 Post Street, San Francisco, CA 94115, USA. E-mail: Steven.Cheung@ucsf.edu

Received April 19, 2020; accepted January 8, 2021; published online ahead of print March 26, 2021.

REFERENCES

Bilecen, D., Seifritz, E., Radü, E. W., Schmid, N., Wetzel, S., Probst, R., Scheffler, K. (2000). Cortical reorganization after acute unilateral hearing loss traced by fMRI. *Neurology*, *54*, 765–767.

Bloom, J. S., & Hynd, G. W. (2005). The role of the corpus callosum in interhemispheric transfer of information: Excitation or inhibition? *Neuropsychol Rev*, *15*, 59–71.

Cai, C., Diwakar, M., Chen, D., Sekihara, K., Nagarajan, S. S. (2019). Robust empirical bayesian reconstruction of distributed sources for electromagnetic brain imaging. *IEEE Trans Med Imaging*, *39*, 567–577.

Carney, E., & Schlauch, R. S. (2007). Critical difference table for word recognition testing derived using computer simulation. *J Speech Lang Hear Res*, *50*, 1203–1209.

Chang, J. L., Huwyler, C. M., Cueva, K. L., Henderson-Sabes, J., Cheung, S. W. (2020). Ear preference and interaural threshold asymmetry. *Otol Neurotol*, *41*, e1178–e1184.

Chang, J. L., Pross, S. E., Findlay, A. M., Mizuiri, D., Henderson-Sabes, J., Garrett, C., Nagarajan, S. S., Cheung, S. W. (2016). Spatial plasticity of the auditory cortex in single-sided deafness. *Laryngoscope*, *126*, 2785–2791.

Cheung, S. W., Atencio, C. A., Levy, E. R. J., Froemke, R. C., Schreiner, C. E. (2017). Anisomorphic cortical reorganization in asymmetric sensorineural hearing loss. *J Neurophysiol*, *118*, 932–948.

Cheung, S. W., Bonham, B. H., Schreiner, C. E., Godey, B., Copenhaver, D. A. (2009). Realignment of interaural cortical maps in asymmetric hearing loss. *J Neurosci*, *29*, 7065–7078.

Code, R. A., & Winer, J. A. (1986). Columnar organization and reciprocity of commissural connections in cat primary auditory cortex (AI). *Hear Res*, *23*, 205–222.

Dalal, S. S., Guggisberg, A. G., Edwards, E., Sekihara, K., Findlay, A. M., Canolty, R. T., Berger, M. S., Knight, R. T., Barbaro, N. M., Kirsch, H. E., Nagarajan, S. S. (2008). Five-dimensional neuroimaging: Localization of the time-frequency dynamics of cortical activity. *Neuroimage*, *40*, 1686–1700.

Dalal, S. S., Zumer, J. M., Guggisberg, A. G., Trumpis, M., Wong, D. D., Sekihara, K., Nagarajan, S. S. (2011). MEG/EEG source reconstruction, statistical evaluation, and visualization with NUTMEG [Research Support, N.I.H., Extramural Research Support, Non-U.S. Gov't]. *Comput Intell Neurosci*, *2011*, 758973.

Douglas, S. A., Yeung, P., Daudia, A., Gatehouse, S., O'Donoghue, G. M. (2007). Spatial hearing disability after acoustic neuroma removal. *Laryngoscope*, *117*, 1648–1651.

Fujiki, N., Naito, Y., Nagamine, T., Shiomi, Y., Hirano, S., Honjo, I., Shibasaki, H. (1998). Influence of unilateral deafness on auditory evoked magnetic field. *Neuroreport*, *9*, 3129–3133.

Guiard, Y. (1980). Cerebral hemispheres and selective attention. *Acta Psychol (Amst)*, *46*, 41–61.

Henshall, K. R., Sergejew, A. A., McKay, C. M., Rance, G., Shea, T. L., Hayden, M. J., Innes-Brown, H., Copolov, D. L. (2012). Interhemispheric transfer time in patients with auditory hallucinations: An auditory event-related potential study. *Int J Psychophysiol*, *84*, 130–139.

Killion, M. C., Niquette, P. A., Gudmundsen, G. I., Revit, L. J., Banerjee, S. (2004). Development of a quick speech-in-noise test for measuring signal-to-noise ratio loss in normal-hearing and hearing-impaired listeners. *J Acoust Soc Am*, *116*(4 Pt 1), 2395–2405.

Kinsbourne, M. (1970). The cerebral basis of lateral asymmetries in attention. *Acta Psychol (Amst)*, *33*, 193–201.

Kitzes, L. M., & Semple, M. N. (1985). Single-unit responses in the inferior colliculus: Effects of neonatal unilateral cochlear ablation. *J Neurophysiol*, *53*, 1483–1500.

Lee, M. Y., Kim, D. H., Park, S. K., Jun, S. B., Lee, Y., Choi, J. J., Yoo, H. J., Raphael, Y., Oh, S. H. (2017). Disappearance of contralateral dominant neural activity of auditory cortex after single-sided deafness in adult rats. *Neurosci Lett*, *657*, 171–178.

Margolis, R. H., & Saly, G. L. (2008). Asymmetric hearing loss: Definition, validation, and prevalence. *Otol Neurotol*, *29*, 422–431.

Niziolek, C. A., Nagarajan, S. S., Houde, J. F. (2013). What does motor efference copy represent? Evidence from speech production. *J Neurosci*, *33*, 16110–16116.

Noble, W., & Gatehouse, S. (2004). Interaural asymmetry of hearing loss, speech, spatial and qualities of hearing scale (SSQ) disabilities, and handicap. *Int J Audiol*, *43*, 100–114.

Owen, J. P., Wipf, D. P., Attias, H. T., Sekihara, K., Nagarajan, S. S. (2012). Performance evaluation of the Champagne source reconstruction algorithm on simulated and real M/EEG data [Comparative Study Research Support, N.I.H., Extramural Research Support, Non-U.S. Gov't Research Support, U.S. Gov't, Non-P.H.S.]. *Neuroimage*, *60*, 305–323.

Ponton, C. W., Vasama, J. P., Tremblay, K., Khosla, D., Kwong, B., Don, M. (2001). Plasticity in the adult human central auditory system: Evidence from late-onset profound unilateral deafness. *Hear Res*, *154*, 32–44.

Popelar, J., Erre, J. P., Aran, J. M., Cazals, Y. (1994). Plastic changes in ipsi-contralateral differences of auditory cortex and inferior colliculus evoked potentials after injury to one ear in the adult guinea pig. *Hear Res*, *72*, 125–134.

Popelář, J., Šuta, D., Lindovský, J., Bureš, Z., Pysanenko, K., Chumak, T., Syka, J. (2016). Cooling of the auditory cortex modifies neuronal activity in the inferior colliculus in rats. *Hear Res*, *332*, 7–16.

Pross, S. E., Chang, J. L., Mizuiri, D., Findlay, A. M., Nagarajan, S. S., Cheung, S. W. (2015). Temporal cortical plasticity in single-sided deafness: A functional imaging study. *Otol Neurotol*, *36*, 1443–1449.

Reale, R. A., & Kettner, R. E. (1986). Topography of binaural organization in primary auditory cortex of the cat: Effects of changing interaural intensity. *J Neurophysiol*, *56*, 663–682.

Rouiller, E. M., Simm, G. M., Villa, A. E., de Ribaupierre, Y., de Ribaupierre, F. (1991). Auditory corticocortical interconnections in the cat: Evidence for parallel and hierarchical arrangement of the auditory cortical areas. *Exp Brain Res*, *86*, 483–505.

Saldaña, E., & Merchán, M. A. (2005). Intrinsic and commissural connections of the inferior colliculus. In J. A. Winer & C. E. Schreiner (Eds.), *The Inferior Colliculus* (pp. 155–181). Springer.

Scally, B., Burke, M. R., Bunce, D., Delvenne, J. F. (2018). Visual and visuomotor interhemispheric transfer time in older adults. *Neurobiol Aging*, *65*, 69–76.

Scheffler, K., Bilecen, D., Schmid, N., Tschopp, K., Seelig, J. (1998). Auditory cortical responses in hearing subjects and unilateral deaf patients as detected by functional magnetic resonance imaging. *Cereb Cortex*, *8*, 156–163.

Shang, Y., Hinkley, L. B., Cai, C., Subramaniam, K., Chang, Y. S., Owen, J. P., Garrett, C., Mizuiri, D., Mukherjee, P., Nagarajan, S. S., Cheung, S. W. (2018). Functional and structural brain plasticity in adult onset single-sided deafness. *Front Hum Neurosci*, *12*, 474.

Silman, S., Gelfand, S. A., Silverman, C. A. (1984). Late-onset auditory deprivation: Effects of monaural versus binaural hearing aids. *J Acoust Soc Am*, *76*, 1357–1362.

Silverman, C. A., & Emmer, M. B. (1993). Auditory deprivation and recovery in adults with asymmetric sensorineural hearing impairment. *J Am Acad Audiol*, *4*, 338–346.

Silverman, C. A., Silman, S., Emmer, M. B., Schoepflin, J. R., Lutolf, J. J. (2006). Auditory deprivation in adults with asymmetric, sensorineural hearing impairment. *J Am Acad Audiol*, *17*, 747–762.

van der Knaap, L. J., & van der Ham, I. J. (2011). How does the corpus callosum mediate interhemispheric transfer? A review. *Behav Brain Res*, *223*, 211–221.

Vannson, N., James, C., Fraysse, B., Strelnikov, K., Barone, P., Deguine, O., Marx, M. (2015). Quality of life and auditory performance in adults with asymmetric hearing loss. *Audiol Neurootol*, *20*(Suppl 1), 38–43.

Wipf, D. P., Owen, J. P., Attias, H. T., Sekihara, K., Nagarajan, S. S. (2010). Robust Bayesian estimation of the location, orientation, and time course of multiple correlated neural sources using MEG. *Neuroimage*, *49*, 641–655.

Yazgan, M. Y., Wexler, B. E., Kinsbourne, M., Peterson, B., Leckman, J. F. (1995). Functional significance of individual variations in callosal area. *Neuropsychologia*, *33*, 769–779.